

A portable smartphone-based imaging surface plasmon resonance biosensor for allergen detection in plant-based milks

Chi Xiao^{a,1}, Georgina Ross^{b,c,1}, Michel W.F. Nielen^{b,c}, Jens Eriksson^a, Gert IJ. Salentijn^{b,c,**}, Wing Cheung Mak^{a,d,*}

^a Division of Sensor and Actuator Systems, IFM – Linköping University, S58183, Linköping, Sweden

^b Wageningen Food Safety Research (WFSR), Wageningen University & Research, P.O. Box 230, 6700, AE, Wageningen, the Netherlands

^c Laboratory of Organic Chemistry, Wageningen University, Helix Building 124, Stippeneng 4, 6708 WE, Wageningen, the Netherlands

^d Department of Biomedical Engineering, The Chinese University of Hong Kong, Shatin, Hong Kong, China

ARTICLE INFO

Handling Editor: Manel del Valle

Keywords:

Portable surface plasmon resonance

Smartphone analysis

Food allergens

Immunoassay

Point of need

Plant-based milk

ABSTRACT

Food allergies are hypersensitivity immune responses triggered by (traces of) allergenic compounds in foods and drinks. The recent trend towards plant-based and lactose-free diets has driven an increased consumption of plant-based milks (PBMs) with the risk of cross-contamination of various allergenic plant-based proteins during the food manufacturing process. Conventional allergen screening is usually performed in the laboratory, but portable biosensors for on-site screening of food allergens at the production site could improve quality control and food safety. Here, we developed a portable smartphone imaging surface plasmon resonance (iSPR) biosensor composed of a 3D-printed microfluidic SPR chip for the detection of total hazelnut protein (THP) in commercial PBMs and compared its instrumentation and analytical performance with a conventional benchtop SPR. The smartphone iSPR shows similar characteristic sensorgrams compared with the benchtop SPR and enables the detection of trace levels of THP in spiked PBMs with the lowest tested concentration of 0.625 µg/mL THP. The smartphone iSPR achieved LoDs of 0.53, 0.16, 0.14, 0.06, and 0.04 µg/mL THP in 10x-diluted soy, oat, rice, coconut, and almond PBMs, respectively, with good correlation with the conventional benchtop SPR system (R^2 0.950–0.991). The portability and miniaturized characteristics of the smartphone iSPR biosensor platform make it promising for the future on-site detection of food allergens by food producers.

1. Introduction

Globally, over 250 million people have immunological hypersensitivity toward food allergens, making the presence of food allergens one of the most prevalent and increasingly relevant food safety issues [1]. Food allergens are typically naturally occurring proteins that are present in foods and drinks. According to EU legislation (Regulation (EU) 1169/2011), food products that contain any of 14 specifically listed allergens as ingredients must explicitly declare so on the packaging [2]. The EU has adopted this zero-tolerance approach to foods known to contain allergens because consumption of even trace amounts of these allergens can cause adverse, sometimes life-threatening effects in sensitive allergic individuals [3,4]. The EU's zero-tolerance approach aims to protect 100% of the allergic population from adverse effects.

However, the threshold level at which allergic reactions occurs differs on an individual and population basis [5]. As such, risk-based clinical thresholds have been proposed that translate minimum eliciting doses of allergens from oral food challenges into the lowest observable adverse effects levels (LOAEL) [6]. These LOAELs, based on the milligrams of total protein from an allergenic food divided by the amount of food consumed, represent the eliciting dose (ED) at which only the most sensitive 5% (ED05) and 1% (ED01) of the allergic population would react with symptoms [7]. Regardless of individual differences in sensitivities towards allergens, it is the presence of undeclared allergens that are accidentally introduced into foods or drinks through cross-contamination, which constitutes the biggest threat to the allergic consumer [8]. A recent investigation on 157 accidental food allergy reactions found that the concentrations of undeclared allergens ranged

* Corresponding author. Department of Biomedical Engineering, The Chinese University of Hong Kong, Shatin, Hong Kong, China.

** Corresponding author. Wageningen Food Safety Research (WFSR), Wageningen University & Research, P.O. Box 230, 6700, AE, Wageningen, the Netherlands.

E-mail addresses: gert.salentijn@wur.nl (G.I.J. Salentijn), wing.cheung.mak@cuhk.edu.hk (W.C. Mak).

¹ First authors.

from 4 to 5000 ppm ($\mu\text{g/mL}$), putting some of these undeclared allergens above clinical EDs based on LOAELs [5,9].

At the same time, there is an ongoing trend in moving towards animal-free, alternative food and drink products. Importantly, in recent years global consumption of lactose has drastically decreased, with cow's milk being widely replaced by plant-based milks (PBMs) [10]. PBMs are water-based extracts made from raw allergenic plant materials such as cereal crops (wheat, oat, rice), tree nuts (hazelnut, almond, coconut), or legumes (soy, peanuts) [10,11]. These raw materials are susceptible to contamination by pesticides, mycotoxins, or bioactive compounds, such as allergens [3]. Even with dedicated sanitation procedures, trace amounts of allergenic proteins can still unintentionally end up in food or drink products [12], with the risk of cross-contamination increasing in facilities that handle or store multiple raw allergenic ingredients. Hazelnut is considered one of the most critical food allergens in Europe; the eliciting doses for hazelnut of 3.5 mg (ED05) and 0.1 mg (ED01) thus requires detection methods in the low ppm ($\mu\text{g/mL}$ or mg/kg) range [7,13,14].

Therefore, to align with the EU's zero-tolerance approach on the food and beverages safety, methods are required that detect allergens as low reasonably achievable (ALARA) [5]. Despite having a rather low ED threshold, in recent years there has been an increase in the use of hazelnut as an ingredient in many foods or drink products owing to its health benefits and desirable flavor profile [15,16].

To improve consumer safety and minimize the occurrence of allergen-related product recalls, it is essential to have rapid and sensitive screening methods that can be carried out by food manufacturers for on-site monitoring of undeclared allergens in their products. Currently, the most widely used methods for food allergen detection include enzyme-linked immunosorbent assay (ELISA) [17] and polymerase chain reaction (PCR) [18]. Although these approaches are very mature, immunological-based ELISAs require multiple assay steps, are time-consuming (taking up to 4 h for standard ELISA protocols [17] sometimes with overnight incubation steps [19]) and typically give LODs between 0.04 and 10 ppm [13]. In contrast, methods that detect allergens at a DNA level, such as PCR, enable the amplification and qualitative detection of specific allergenic (i.e., detects the presence or absence of a specific DNA sequence) and can be combined with complementary methods, such as real-time PCR to give quantitative detection of specific sequences with LODs between 0.1 and 100 ppm [20]. Still, such methods use complicated DNA sample preparation, purification, and probe-based analysis procedures, requiring multiple hands-on steps making them very time consuming [21]. These methods have limited applicability for on-site testing by untrained users, and do not meet the need for simplified, rapid, ubiquitous, screening methods that allow for the immediate detection of allergens at all stages of PBM production/storage. More recently, biosensors with various transduction technologies based on electrochemical [22], immunochemical [23], electromechanical [24], and optical [25] platforms have been developed for the rapid detection of allergens. These developments are strengthened by the parallel technological advances in smartphones and 3D printing, which have inspired new research to explore various built-in electronic and optical features for their applicability in portable smartphone-based biosensors [26]. The ubiquity of devices with touch-sensitive screens, internet connectivity, and powerful Central Processing Units (CPUs), together with their integrated optical elements including Light Emitting Diodes (LEDs) and high-performance cameras make smartphones suitable for portable plasmonic sensing applications based on fiber-optics [27,28], prism coupling [29], grating [30], and plasmonic nanostructures [31,32].

A particularly powerful biosensing strategy is surface plasmon resonance (SPR), which has been applied to quantitative food allergen detection due to its high sensitivity and label-free detection mechanism [33–35]. However, conventional, benchtop SPR instruments are restricted to the laboratory, owing to their cost, bulky size, need for regular maintenance, and the necessity of trained personnel for their

operation, thus limiting their on-site applicability [36]. A major challenge in addressing the size and portability of SPR instruments is miniaturizing the complex fluidic handling unit present in the benchtop system [37,38]. Most commonly, polydimethylsiloxane (PDMS)-based soft lithography is used to manufacture customized microfluidics for portable SPR systems, but such fabrication is labor-intensive and requires a clean-room environment [39–42]. Previously, the user-friendliness and on-site applicability of a smartphone were leveraged to develop a portable imaging SPR (iSPR) biosensor to facilitate moving SPR out of the lab and to the point-of-need (PoN) [43].

Here, we report the development of a sensitive and specific direct SPR immunoassay for the quantitative analysis of total hazelnut protein (THP) in 5 different PBMs (rice, oat, almond, coconut, and soy). After initial development using a benchtop SPR platform, we implemented the same immunoassay on a portable smartphone-based iSPR platform and benchmarked its analytical performance as a semi-quantitative screening method against its commercial quantitative counterpart in terms of sensitivity and future potential as an on-site allergen screening method for the food industry.

2. Materials & methods

2.1. Materials

Anti-hazelnut (50-6B12) and anti-peanut (51-2A12) monoclonal antibodies (mAbs) were developed at Wageningen Food Safety Research (WFSR) [35] and were selected in previous studies by SPR for their speed, sensitivity, and specificity towards total hazelnut protein (THP) and specificity towards total peanut protein (TPP) [8,44]. An amine coupling kit (containing 0.1 M N-hydroxysuccinimide (NHS), 0.4 M 1-ethyl-3-(3-dimethylaminopropyl)carbodiimide hydrochloride (EDC), and 1 M ethanolamine hydrochloride (pH 8.5), a pH scouting kit (containing 10 mM sodium acetate pH 4.0, 4.5, 5.0 & 5.5), HBS-EP buffer (pH 7.4, consisting of 10 mM 4-(2-hydroxyethyl)piperazine-1-ethanesulfonic acid, 150 mM sodium chloride, 3 mM ethylenediaminetetraacetic acid, 0.005% v/v surfactant polysorbate-20), CM5 sensor chips and regeneration solution (10 mM glycine-HCl, pH 1.75) were purchased from GE Healthcare (Uppsala, Sweden). All solutions were prepared with MQ water from a MilliQ-system ($>18.2 \text{ M}\Omega/\text{cm}$). A syringe pump was purchased from New Era Pump Systems, Inc (NY, USA). A white LED backlight module (model: 1626) was purchased from Adafruit Industries (NY, USA). A smartphone (Samsung Galaxy A5) was purchased from Samsung Electronics Co., Ltd. (Seoul, South Korea).

2.2. Plant based milk sample preparation

Rice (13.8%), oat (9.8%), almond (2.3%), coconut (5.3%), and soy (8.7%) PBMs were purchased from local supermarkets (see Supplementary Information (SI), Table S1 for ingredient lists). Before SPR analysis, the PBMs were diluted at 1:9 (v/v) in HBS-EP running buffer (RB). The packaging of the PBMs did not state to contain any hazelnut or other tree nuts and the 1:9 diluted PBMs served as the 'blank' or unspiked matrices. To confirm these samples were free from hazelnuts, the diluted PBMs were first analyzed using the sensitive benchmark assay. Certified standardized reference materials for food allergens are not widely available and require in-house preparation. Total hazelnut protein (THP) extracts were prepared as described previously [45]. The THP extract was diluted to 100 $\mu\text{g/mL}$ in RB and used to spike RB and the diluted PBMs at concentrations of 20, 10, 5, 2.5, 1.25, 0.625 $\mu\text{g/mL}$ for iSPR experiments and 20, 10, 5, 2.5, 1.25, 0.625, 0.312 and 0.125 $\mu\text{g/mL}$ for benchtop SPR experiments. These concentrations (7 data points plus a blank for the iSPR experiments, or 10 data points plus a blank for the benchtop SPR experiments) of THP spiked into PBMs were selected to represent trace levels of allergens that could be accidentally introduced into foods by cross-contamination. The assay would also be

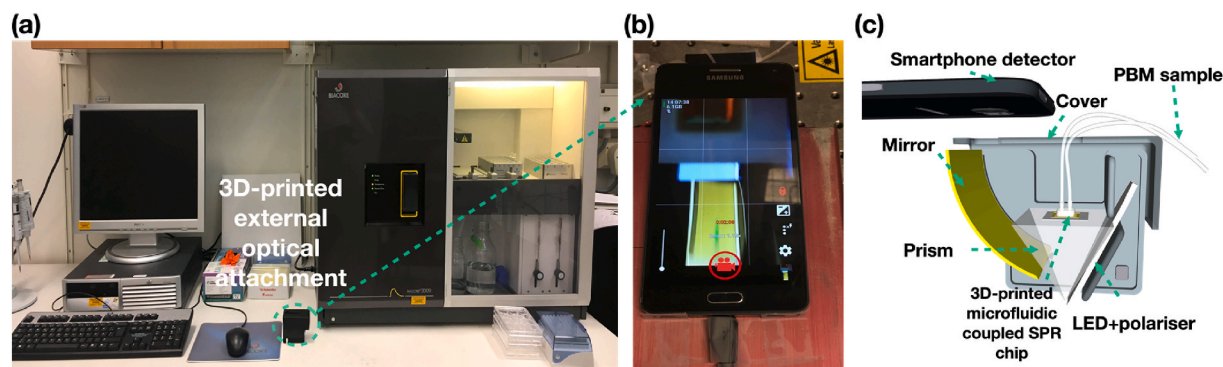


Fig. 1. (a) Photograph of the actual size comparison between the benchtop SPR and smartphone iSPR systems. (b) Photograph of the actual optical attachment integrated with a smartphone. (c) Schematic of the prototype smartphone iSPR platform.

capable of testing higher concentrations of THP (i.e., $>20 \mu\text{g/mL}$), but these higher concentrations might first require dilution before analysis to put them into the dynamic working range for this assay.

2.3. Benchtop SPR

All benchtop SPR experiments were carried out using a BIACORE 3000 (GE Healthcare, Uppsala, Sweden).

2.4. SPR chip preparation

Anti-hazelnut mAb was immobilized onto the CM5 chip using a standard amine coupling procedure at 25°C . First, to determine the optimum immobilization pH, antibodies were diluted to $100 \mu\text{g/mL}$ in 10 mM sodium acetate (pH 4.0–5.0). The optimal immobilization response was reached at pH 4.5. The four flow cells (FCs) pressed against the carboxymethylated (CM) dextran chip surface, were simultaneously activated by injecting $35 \mu\text{L}$ of a mixture of EDC and NHS (1:1; v/v) at a flow rate of $5 \mu\text{L/min}$. Anti-peanut mAb (51-2A12) was immobilized in the reference FC (FC1) to correct for non-specific binding [44] and anti-hazelnut mAb (50-6B12) was immobilized in the measurement FC (FC2). After coupling, the remaining active carboxylic acid sites were blocked by injecting ethanolamine (1 M).

2.5. Direct total hazelnut protein immunoassay

Each 10x-diluted and THP-spiked ($0.125\text{--}20 \mu\text{g/mL}$) PBM sample was tested at 25°C across different days, in triplicate. Analysis was performed by injecting $10 \mu\text{L}$ of sample into both FCs, at a flow rate of $20 \mu\text{L/min}$ and monitoring the binding response in both FCs. To regenerate the surface, $10 \mu\text{L}$ of 10 mM NaOH was injected at a flow rate of $20 \mu\text{L/min}$. The total analysis run time, including sample and regeneration injections, was 5 min per sample.

2.6. Data processing for benchtop SPR

To process the data, sensorgrams were superimposed, aligned on the x-axis at the sample injection point, aligned on the y-axis to the baseline, and the regeneration curves were removed using the Biaevaluation software (Uppsala, Sweden). The sensorgrams were corrected by using FC1 as a control channel and subtracting the FC1 response from the FC2 response. The association and dissociation data allowed a visual comparison to be made between the different THP concentrations per PBM ($n = 3$). Subsequently, a calibration curve was constructed by plotting the final response units (RUs) following sample injection (approx. after 30 s) against THP concentration to quantitatively compare the binding responses at all THP concentrations in the different PBMs. The limit of detection (LOD) was determined as $3 \times$ standard deviation of the blank divided by the slope of the calibration curve [46].

2.7. Smartphone-based imaging SPR (iSPR)

2.7.1. Integrated iSPR platform

The portable iSPR platform and microfluidics were produced and used according to the previously reported design and protocol [43]. Fig. 1 presents the schematic design and the actual image of the smartphone-based iSPR system, next to the benchtop instrument. All computer-aided designs (CAD) were created using the Autodesk software (Autodesk Inventor Fusion, Autodesk Inc, USA). The CAD file for the microfluidic chip was converted into the STL file format, imported to the 3D printer software PreForm3 (PreForm 3; Formlabs Inc, USA), and printed with a Form 3 printer (Formlabs Inc, USA) using clear resin (Clear Type O4, Formlabs Inc, USA) at $25 \mu\text{m}$ layer thickness. The CAD files for the portable iSPR platform, consisting of an inner body for mounting the light source, prism optics, and a top cover for smartphone attachment were imported as STL files, into the Ultimaker Cura slicer software (Ultimaker Cura v.4.13.1) and converted to G-code before being printed by fused deposition modeling (FDM) 3D printer (Hephestos 2, BQ, Spain) with polylactic acid (PLA) filament with $200 \mu\text{m}$ layer thickness. The smartphone iSPR instrument consisted of an external attachment that served as an optical bench for the alignment of the prism, mirror, and a LED light source with the Kretschmann arrangement for guiding the iSPR optics. For the assembly of the smartphone iSPR platform, a commercial BK7 60° prism was installed in the center of the 3D-printed inner body as the light guide. A white LED coupled with a polarizer was installed at the incident light side of the prism used to provide a plane-polarized light source for iSPR, whereas a curved polished mirror was installed at the reflected light side of the prism to direct the output light signal to the smartphone camera. To perform smartphone iSPR measurement, the 3D-printed microfluidics-coupled SPR chip was placed on the prism surface with a layer of immersion oil, and the inlet and outlet of the SPR microfluidic chips were connected via silicon tubings and closed with a 3D-printed cover. The outer surfaces of the printed attachment were coated with matte black paint (Biltema, Sweden) to shield the interior from environmental light. The incident polarized LED was directed by the prism to the SPR sensor surface, where the reflected light resulting from the SPR angle shift was guided by the prism and projected onto a mirror, forming an SPR image that could be detected by the smartphone camera.

2.8. SPR chip preparation

For the preparation of an integrated microfluidic SPR sensing chip, the 3D-printed microfluidics was attached to the gold sensing surface of the CM5 chips using double-sided adhesive tape (Biltema, Sweden) with an open window ($0.5 \times 2.7 \text{ mm}$) that followed the width and length of the microfluidic channel created by laser cutter using vector mode at a power of 56% (5th Generation Full Spectrum, Las Vegas, USA). For the biofunctionalization of the microfluidic SPR chip, reagents were loaded

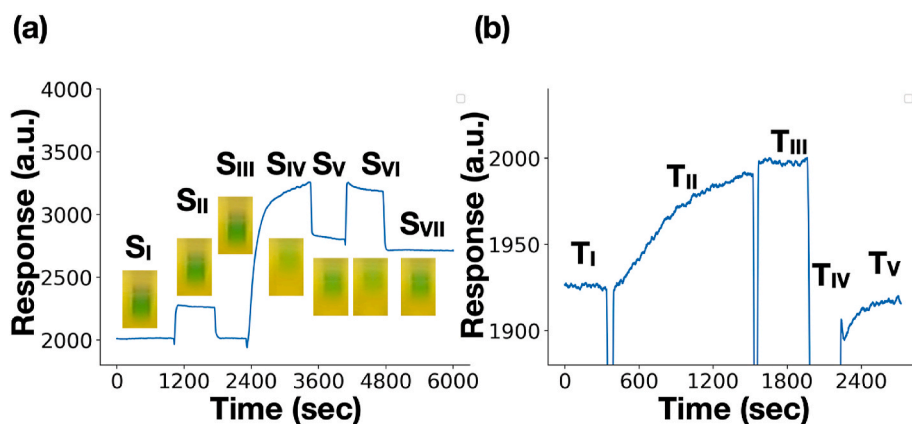


Fig. 2. (a) Sensorgram of the smartphone iSPR for the immobilization of monoclonal anti-hazelnut Ab. The insets show the positions of the iSPR signal (the green band, which contains a 200×10 pixels area, represents the region of interest (ROI) captured from the SPR video frame [43]) measured by the smartphone camera. The sensorgram shows the activation of the carboxyl-dextran with EDC/NHS (S_{II}), the coupling of anti-hazelnut mAb (S_{IV}), and the blocking with ethanolamine (S_{VI}), as well as the running buffer HBS-EP steps (S_I , S_{III} , S_V , and S_{VII}). (b) Sensorgram of 10x-diluted blank PBM sample (T_I), injection of total hazelnut protein (THP; 20 $\mu\text{g/mL}$) spiked into running buffer (RB) (T_{II}), running buffer (T_{III}), followed by the surface regeneration with 10 mM glycine-HCl (T_{IV}) to return the signal to baseline (T_V) in smartphone iSPR platform.

into the iSPR system via syringe pumps, and the immobilization process was monitored by the smartphone iSPR platform. A standard amine coupling procedure was applied to immobilize the anti-hazelnut antibody to the CM5 sensor chip. First, HBS-EP was injected as a running buffer for 15 min to establish a stable baseline. A freshly prepared amine-coupling solution composed of a 1:1 v/v mixture of EDC (400 mM) and NHS (100 mM) was injected into the SPR chip at a flow rate of 40 $\mu\text{L/min}$ for 12 min, followed by the injection of HBS-EP buffer at a flow rate of 40 $\mu\text{L/min}$ for 10 min as washing step. Then, the anti-hazelnut antibody with a concentration of 100 $\mu\text{g/mL}$ in 10 mM sodium acetate (pH 4.5) was injected at a flow rate of 40 $\mu\text{L/min}$ for 20 min, followed by the removal of the unbound antibody by washing with the HBS-EP buffer at a flow rate of 40 $\mu\text{L/min}$ for 10 min. Finally, the remaining active sites were blocked by injecting ethanolamine (1 M) at a flow rate of 40 $\mu\text{L/min}$ for 12 min, followed by a washing step with HBS-EP at a flow rate of 40 $\mu\text{L/min}$ for 20 min.

2.9. Direct total hazelnut protein immunoassay

Each 10x-diluted THP-spiked PBM was tested across different days in triplicate with HBS-EP as the running buffer (RB), at room temperature and with a 25 $\mu\text{L/min}$ flow rate. After an initial injection of HBS-EP for 10 min and sequentially the injection of the unspiked sample for 10 min, each PBM spiked with THP (0.625–20 $\mu\text{g/mL}$) was injected via syringe pump into the 3D-printed flow cells for 20 min. Subsequently, HBS-EP was injected for 10 min, followed by an injection of 10 mM glycine-HCl (pH 1.75) for 3 min to regenerate the functionalized surface. The smartphone was attached to the 3D-printed iSPR system and Open-Camera (v1. 45.2) was used to record videos of the chip for the total assay duration.

2.10. Data processing for smartphone iSPR

For data processing, the smartphone videos were exported to a custom python program. In the program's graphical user interface (GUI), the user can manually select the regions of interest (ROIs) on the chip and adjust the width, height, x, and y coordinates of the original frame, and filter order. After checking the SPR curve is complete, the sensorgram from the entire video recording is displayed by clicking 'compute' in the GUI. The assay data were exported and averaged and calibration curves were plotted to quantitatively compare the binding responses at all THP concentrations in the different PBMs. To compare the results from the benchtop SPR and portable iSPR systems for each PBM, correlation analysis was applied to datasets from each platform followed by linear regression (95% confidence) of the correlated results.

3. Results & discussion

Instrumentation, chip preparation, and sensorgram characteristics for benchtop SPR vs. smartphone iSPR.

The smartphone iSPR platform (Fig. 1b) developed in our group [43] is lightweight and portable. The benchtop SPR is 965 times larger in volume than the smartphone iSPR and weighs 360 times more (Fig. 1a). The miniaturized and portable smartphone iSPR platform features an innovative and affordable 3D-printed microfluidics-coupled SPR chip. The microfluidic-coupled chip inserts into a 3D-printed internal attachment on top of the horizontally-aligned prism surface. The surface receives incident light from the polarized LED light source, enabling direct detection of the shift in SPR angle by the reflection of light to the smartphone camera (Fig. 1c).

Antibody immobilization using the smartphone iSPR platform was monitored by tracking the shifting position of the green band from the recorded smartphone iSPR videos (Fig. 2a). The sensorgram shows the successful activation of the carboxyl-dextran with EDC/NHS (S_{II}), the coupling of anti-hazelnut mAb (S_{IV}), and the blocking with ethanolamine (S_{VI}), as well as the washing steps (S_I , S_{III} , S_V , and S_{VII}). The smartphone iSPR sensorgram resolves all the stepwise molecular-interaction characteristics for chip preparation comparably to the benchtop SPR (see SI, Fig. S1 for the immobilization sensorgram from the benchtop SPR). Fig. 2b presents the sensorgram for the detection of THP, which shows a typical association curve (T_{II}) upon injection of the analyte, followed by the dissociation curve (T_{III}) upon injection of buffer solution. Finally, the microfluidic SPR chip was regenerated by the injection of glycine-HCl (T_{IV}), (see Fig. S2 for the regeneration sensorgram using the benchtop SPR platform). This result demonstrates that the smartphone iSPR yields a characteristic sensorgram that is similar to the one obtained with the benchtop SPR instrument (SI, Fig. S2) for the study of biomolecular affinity interaction.

3.1. Matrix effect evaluation and correction

Matrix effects from complex samples may affect the analytical performance in two ways: (i) it may influence the specific binding in the assay, and (ii) lead to non-specific signal responses that contribute to the background signal. Therefore, it is important to evaluate the background signal in PBM food samples and adjust the baseline to minimize such matrix effects. Most commonly, minor non-specific binding and refractive index effects in SPR are compensated by the use of a reference channel for correction, but they can also be alleviated by adjusting the buffer pH, adding protein blockers, using non-ionic surfactants, or increasing salt concentration. Reference surfaces are particularly useful to correct for non-specific adsorption and matrix effect when analyzing trace amounts of food proteins, such as THP, in complex matrices such as the PBMs. The assay on the benchtop SPR uses a reference channel for

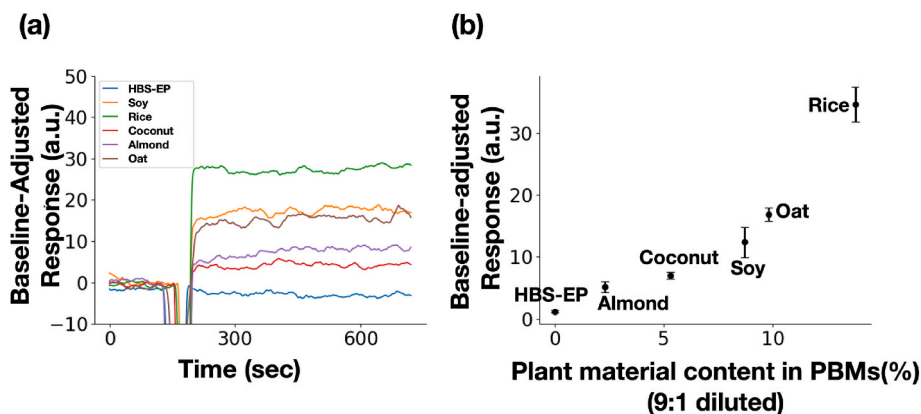


Fig. 3. Matrix effect in different plant-based milk samples. (a) Sensorgram of five unspiked PBM samples. (b) Correlation plot between PBM content and smartphone iSPR baseline adjustment response after 9:1 dilution of the PBM ($n = 3$, error bars represent the standard deviation).

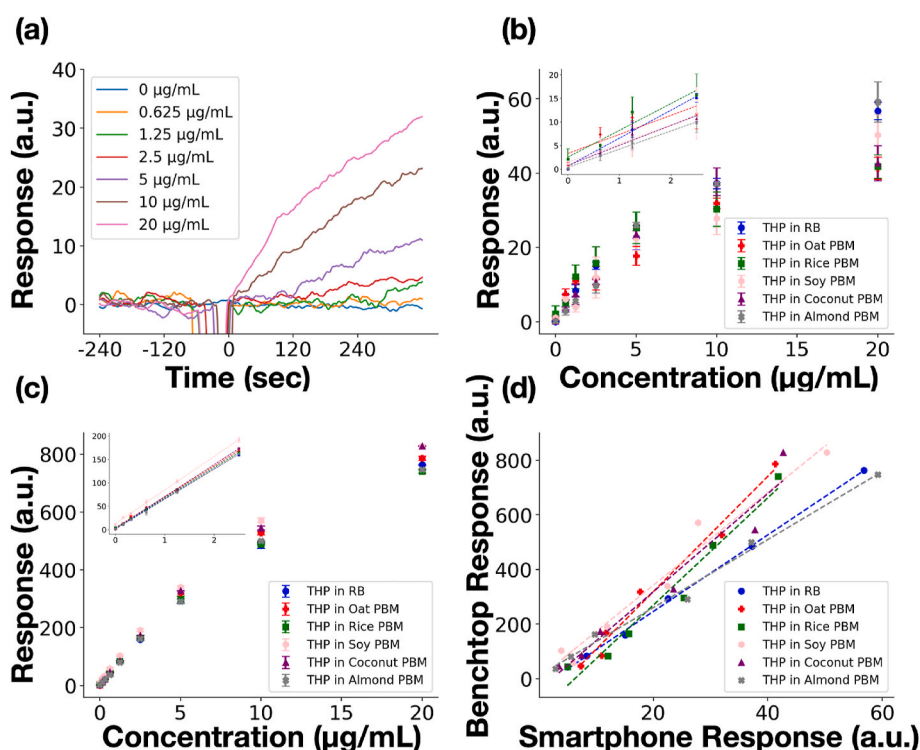


Fig. 4. Performance evaluation of both SPR systems. (a) Sensorgrams were obtained for different concentrations of THP in the range of 0–20 $\mu\text{g/mL}$ in 10x diluted coconut milk in the smartphone iSPR platform. Calibration curves are shown for the detection of total hazelnut protein (THP; 0–20 $\mu\text{g/mL}$; inset shows 0–2.5 $\mu\text{g/mL}$) in different 10x-diluted PBMs using (b) the prototype SPR smartphone, and (c) the benchtop SPR – and (d) their correlation is plotted. Error bars represent the standard deviation ($n = 3$).

parallel blank subtraction, allowing for monitoring of matrix effects and correction of the signal in the measurement channel. As mentioned in the experimental section (PBM sample preparation), certified reference materials for food allergens are not widely available and require in-house preparation. The unspiked samples used here are diluted PBMs that have no declared hazelnut content on their ingredient lists (see SI Table S1). Before spiking with THP, all blank PBM samples were checked using the benchmark SPR assay and, indeed, none were found to contain THP at a concentration detectable by the assay.

The smartphone iSPR prototype does not have a reference channel, and instead, it uses a single-channel design with sequential injections to characterize and correct for matrix effects (see SI, Fig. S3). Matrix effects from the PBMs were observed in the smartphone iSPR-based assay, (see Fig. 3a). The blank signals recorded by the smartphone iSPR can be correlated to the plant content of the corresponding diluted PBM samples, which enables us to understand the complexity of the PBM matrix and achieve baseline adjustment. Fig. 3b presents the correlation plot between the listed plant material content in different PBM samples and

their corresponding blank PBM response in smartphone-based SPR.

3.2. Benchtop SPR vs smartphone iSPR for allergen detection in plant based milks

To ascertain the appropriateness of the smartphone iSPR system for food allergen detection, the direct THP immunoassay was performed on both SPR platforms to compare their analytical performance. The immobilized anti-hazelnut mAb has high affinity and rapid association to THP, allowing THP to be selectively captured in all PBM matrices using both SPR platforms. The overlaid sensorgrams of smartphone iSPR for the quantitative measurement of THP in coconut PBM are presented in Fig. 4a, which shows a fast initial response time (i.e. the rate of the affinity binding, which is related to the analyte concentration) similar to the benchtop SPR sensorgrams (SI, Fig. S4). However, after injection of the sample, faster steady-state responses were observed in the benchtop SPR sensorgrams (within approximately 30 s), while the smartphone iSPR remains in the response region even after 360 s. This might be

Table 1
Assay LOD comparison using both SPR platforms.

Matrix	Benchtop SPR LOD ($\mu\text{g/mL}$)	Prototype iSPR LOD ($\mu\text{g/mL}$)
RB	0.02	0.06
Rice	0.04	0.14
Oat	0.02	0.16
Coconut	0.03	0.06
Almond	0.04	0.04
Soy	0.03	0.53

attributed to the larger sample chamber volume (~ 75 times) of the 3D-printed fluidic chip used in the smartphone iSPR ($0.5 \times 2.7 \times 1.5 \text{ mm}^3$) compared with the fluidic system used in the benchtop SPR ($0.5 \times 2.4 \times 0.02 \text{ mm}^3$) that operates at a similar sample injection rate of $25 \mu\text{L/mL}$ (smartphone iSPR) compared to the $20 \mu\text{L/mL}$ of the benchtop SPR, resulting in a prolonged time to reach the steady-state. See Fig. S5 for a schematic depicting the integrated microfluidic system of each platform.

Calibration curves were constructed by plotting the concentrations of THP (0–20 $\mu\text{g/mL}$) spiked into 10x-diluted PBM against the response after a 10-min PBM injection from the smartphone iSPR (Fig. 4b) and plateau response (i.e., total THP bound following association) from the benchtop SPR after 30 s of PBM injection (Fig. 4c). In the linear range (0–2.5 $\mu\text{g/mL}$), the assay on the benchtop SPR platform showed good linearity ($R^2 = 0.999$) and the iSPR platform showed moderate linearity ($R^2 = 0.757$ – 0.994), with both assays correlating well ($R^2 = 0.960$ – 0.991) as can be seen in Fig. S6 and Table S2. Besides, the smartphone iSPR analyses were performed during a period of more than one month with several reproduced SPR chips to complete all the analyses, which illustrates the reproducibility of the smartphone iSPR method.

The assay on the benchtop SPR platform had a wider dynamic working range and lower LOD, with the lowest concentration tested being $0.125 \mu\text{g/mL}$ compared with $0.625 \mu\text{g/mL}$ on the smartphone iSPR platform (see Table 1 for a summary of results). Still, regardless of the SPR platform used, the reported LODs are sufficiently sensitive to protect the allergic population based on LOAELs at ED05 and ED01 [5]. Moreover, these LODs are consistent with those reported for commercially available hazelnut detection immunoassays (PCR/ELISA/lateral flow), and proof-of-concept SPR immunosensors which have reported detection limits ranging from 0.04 to $10 \mu\text{g/mL}$ [13]. Still it is difficult to compare detection limits from different allergen immunosensors as these vary widely depending on whether the sensors target the total protein extract or individual allergenic protein.

Furthermore, as shown in Fig. 4b, the signal responses from the smartphone iSPR are proportional to the concentration of THP in different PBM samples and RB. However, especially at higher concentrations, the response approaches a plateau, and the responses slightly vary between different PBMs to an extent that is not observed at the lower concentrations. This is likely because, at higher concentrations, binding sites of the immobilized anti-hazelnut antibody are mostly

occupied by THP, preventing further binding. This observation is consistent with the literature on SPR analysis of allergens in foods [47]. Compared to Fig. 4b, the calibration curves of the benchtop SPR (Fig. 4c) have similar increasing trends as those obtained with smartphone-based SPR from 0 to $20 \mu\text{g/mL}$. However, the variation between the calibration curves of different PBM samples is smaller on the benchtop SPR instrument, as is the standard deviation of the measurements themselves, resulting in lower RSD in PBMs at all tested concentrations compared with the prototype smartphone iSPR system (see Table 2).

To further compare the performance of the smartphone iSPR screening method and the quantitative benchtop SPR, the correlation between both platforms was plotted (Fig. 4d). The two methods show good R^2 values for the measurement of oat, rice, soy, coconut, and almond PBMs in the concentration range of 0.625 – $20 \mu\text{g/mL}$, which were 0.984 , 0.960 , 0.965 , 0.95 , and 0.991 , respectively (Fig. S6). These results demonstrate the feasibility and practicality of the portable smartphone iSPR for allergen detection in PBMs. To limit the occurrence of allergen-related PBM recalls, food manufacturers must be able to regularly screen products, production lines, and shared equipment, on-site, for trace allergens, but commercial benchtop SPR biosensors are expensive, laboratory-based, and are unsuitable for general users. Given the affordability and miniaturized features of the smartphone iSPR system, the analytical performance for the detection of THP in PBMs is satisfactory when compared with the benchtop SPR instrument.

Nevertheless, the smartphone iSPR platform is still a prototype and further improvements are needed to reach the same analytical performance as the benchtop SPR system. The detection principle of the iSPR system is based on an imaging technique measured at a fixed angle in Kretschmann's configuration [42,43], which inherently has a relatively lower sensitivity and resolution compared with the conventional SPR configuration [44]. Moreover, the benchtop SPR signal is measured with a highly sensitive, but expensive, photodetector, while the smartphone iSPR is equipped with an economic CMOS camera [45]. The smartphone camera already gives a satisfactory performance and advances in the quality of smartphone cameras are anticipated to further enhance the sensitivity and improve the performance in future iSPR prototypes. The LOD and RSD are related to the standard deviation of the measurements which are affected by the fluidic unit and sample injection procedures. The smartphone iSPR is equipped with a low-cost 3D-printed fluidic chip attached to the SPR gold sensing surface via an adhesive tape, compared with the meticulous automated fluidic and docking system in the benchtop SPR, providing a precise operation in sample injection and a smoother baseline. In future versions of the prototype, an advanced design of the 3D-printed clip-type fluidic cell with an o-ring may refine the attachment and alignment of the fluidic unit and SPR sensing surface. It is expected that further prototyping of the iSPR platform will improve the reusability of the SPR chip so that it can be regenerated and reused for a similar amount of cycles compared with the benchtop system, which can be reused for over 120 cycles (see Fig. S7). The overall instrumental comparison between smartphone iSPR and benchtop SPR

Table 2
Assay relative standard deviation (RSD) for all Plant Based Milks at all tested concentrations on both SPR platforms.

Conc ($\mu\text{g/mL}$)	RB RSD (%)		Rice RSD (%)		Oat RSD (%)		Coconut RSD (%)		Almond RSD (%)		Soy RSD (%)	
	SPR	iSPR	SPR	iSPR	SPR	iSPR	SPR	iSPR	SPR	iSPR	SPR	iSPR
20	0.18	4.21	0.80	7.59	0.96	7.32	0.21	11.08	0.27	9.25	0.49	11.05
10	2.08	3.86	0.41	15.27	1.13	4.51	1.25	9.77	0.28	0.87	1.63	15.57
5	2.37	14.42	4.22	16.71	2.73	14.46	0.43	4.66	2.80	3.22	1.42	14.33
2.5	1.69	6.27	0.79	28.17	3.37	27.04	0.73	5.48	0.94	20.20	2.55	46.16
1.25	1.56	19.18	3.94	29.29	2.09	6.53	2.68	37.10	3.84	23.31	3.22	32.47
0.625	3.63	46.65	6.13	16.78	6.86	19.92	1.28	11.07	15.05	38.47	8.17	10.01
0.312	5.30	n/a ^a	11.71	n/a ^a	10.21	n/a ^a	4.99	n/a ^a	9.19	n/a ^a	6.97	n/a ^a
0.156	9.14	n/a ^a	5.57	n/a ^a	13.52	n/a ^a	5.54	n/a ^a	22.06	n/a ^a	6.29	n/a ^a
0	50.70	85.30	13.32	135.98	108.6	29.60	33.11	68.36	25.0	6.24	14.78	153.27

*RSD calculated as $100 \times \text{standard deviation/average}$.

^a Not tested at this concentration.

Table 3

Comparison of instrument parameters across both SPR platforms.

INSTRUMENT PARAMETER	BENCHTOP SPR	SMARTPHONE-iSPR
Instrument cost (\$)	100 k	~100
Weight	50 kg	138 g
Dimensions (L × W × H)	760 × 350 × 610 mm	70 × 60 × 40 mm
Electric voltage	100–120 V; 220–240 V	9 V
Power consumption	max 580 VA	2900 MAh
Automation	Autosampler	Manual operation ^a
Data processing	Biaevaluation	Python Program ^a
Sample volume/injection	10 µL	250 µL ^a

^a Limited by current prototypical design, but are expected to be brought up to par by product engineering.

is given in Table 3.

4. Conclusion

This study demonstrated the development of an affordable direct immunoassay for the real-time detection of total hazelnut protein in 5 different plant-based milks with sensitivity comparable to or better than commercially available hazelnut immunoassays and proof-of-concept SPR-based immunosensors. A direct comparison of the platform parameters for the detection of THP in PBMs has been summarized in Tables 1–3. Ultimately, while improvements can still be made to the platform's usability, portability, assay duration, re-usability, and throughput capacity for food allergen detection applications, the current iSPR prototype yields commendable sensitivity, at only a fraction of the cost and size of a conventional commercial desktop SPR platform, making it promising as an alternative, affordable, portable sensing platform for decentralized allergen screening in PBMs.

Author contributions

C.X. designed and performed the smartphone iSPR experiments, data analysis and wrote the corresponding sections of the manuscript. G.M.S. R. designed and optimized the immunochemistry, prepared the PBMs samples, performed benchtop SPR experiments, data analysis and wrote the corresponding sections of the manuscript. M.W.F.N. acquired project, revised the manuscript. J.E. supervised the development of smartphone iSPR, food sample analysis and revised the manuscript. G. I.J.S. supervised the research on antibodies biochemistry, assay development, benchtop SPR analysis and revised the manuscript. W.C.M. supervised the development of smartphone iSPR, assay optimization, food sample analysis and revised the manuscript. All authors approved the final version of the manuscript.

Declaration of competing interest

The authors declare that they have no known competing financial interests or personal relationships that could have appeared to influence the work reported in this paper.

Data availability

Data will be made available on request.

Acknowledgements

The authors would like to acknowledge the European Union's Horizon 2020 research and innovation program under the Marie Skłodowska-Curie grant agreement No. 720325 for generous financial support to carry out this research.

Appendix A. Supplementary data

Supplementary data to this article can be found online at <https://doi.org/10.1016/j.talanta.2023.124366>.

References

- [1] R.C. Alves, M.F. Barroso, M.B. González-García, M.B. Oliveira, C. Delerue-Matos, New trends in food allergens detection: toward biosensing strategies, *Crit. Rev. Food Sci. Nutr.* 56 (2016) 2304–2319.
- [2] I. Reese, T. Holzhauser, S. Schnadt, S. Dölle, J. Kleine-Tebbe, M. Raithe, M. Worm, T. Zuberbier, S. Vieths, Allergen and allergy risk assessment, allergen management, and gaps in the European Food Information Regulation (FIR): are allergic consumers adequately protected by current statutory food safety and labelling regulations? *Allergo J Int* 24 (2015) 180–184.
- [3] J.M. Soon, L. Manning, May Contain" allergen statements: facilitating or frustrating consumers? *J. Consum. Pol.* 40 (2017) 447–472.
- [4] I.J. Skypala, Food-induced anaphylaxis: role of hidden allergens and cofactors, *Front. Immunol.* 10 (2019) 673.
- [5] C.B. Madsen, M.W. van den Dungen, S. Cochrane, G.F. Houben, R.C. Knibb, A. C. Knulst, S. Ronsmans, R.A.R. Yarham, S. Schnadt, P.J. Turner, J. Baumert, E. Cavandoli, C.H. Chan, A. Warner, R.W.R. Crevel, Can we define a level of protection for allergic consumers that everyone can accept? *Regul. Toxicol. Pharmacol.* 117 (2020), 104751.
- [6] S. Taylor, S. Hefle, C. Bindslev-jensen, F. Atkins, C. Andre, C. Bruijnzeel-koomen, A. Burks, R. Bush, M. Ebisawa, P. Eigenmann, A consensus protocol for the determination of the threshold doses for allergenic foods: how much is too much? *Clin. Exp. Allergy* 34 (2004) 689–695.
- [7] B.C. Remington, J. Westerhout, M.Y. Meima, W.M. Blom, A.G. Kruizinga, M. W. Wheeler, S.L. Taylor, G.F. Houben, J.L. Baumert, Updated population minimal eliciting dose distributions for use in risk assessment of 14 priority food allergens, *Food Chem. Toxicol.* 139 (2020), 111259.
- [8] G.M.S. Ross, M.G.E.G. Bremer, J.H. Wichers, A. van Amerongen, M.W.F. Nielen, Rapid antibody selection using surface plasmon resonance for high-speed and sensitive hazelnut lateral flow prototypes, *Biosensors* 8 (2018).
- [9] W.M. Blom, A.D. Michelsen-Huisman, H. van Os-Medendorp, G. van Duijn, M.L. de Zeeuw-Brouwer, A. Versluis, J.J.M. Castenmiller, H.P.J.M. Noteborn, A. G. Kruizinga, A.C. Knulst, G.F. Houben, Accidental food allergy reactions: products and undeclared ingredients, *J. Allergy Clin. Immunol.* 142 (2018) 865–875.
- [10] E.F. Aydar, S. Tutuncu, B. Ozcelik, Plant-based milk substitutes: bioactive compounds, conventional and novel processes, bioavailability studies, and health effects, *J. Funct. Foods* 70 (2020), 103975.
- [11] P.E.S. Munekata, R. Domínguez, S. Budaraju, E. Roselló-Soto, F.J. Barba, K. Mallikarjunan, S. Roohinejad, J.M. Lorenzo, Effect of innovative food processing technologies on the physicochemical and nutritional properties and quality of non-dairy plant-based beverages, *Foods* 9 (2020).
- [12] F.D. Europe, Guidance on Food Allergen Management for Food Manufacturers, 2013. Belgium, www.fooddrinkurope.eu.
- [13] G.M.S. Ross, M.G.E.G. Bremer, M.W.F. Nielen, Consumer-friendly food allergen detection: moving towards smartphone-based immunoassays, *Anal. Bioanal. Chem.* 410 (2018) 5353–5371.
- [14] G.F. Houben, J.L. Baumert, W.M. Blom, A.G. Kruizinga, M.Y. Meima, B. C. Remington, M.W. Wheeler, J. Westerhout, S.L. Taylor, Full range of population Eliciting Dose values for 14 priority allergenic foods and recommendations for use in risk characterization, *Food Chem. Toxicol.* 146 (2020), 111831.
- [15] T. Weinberger, S. Sicherer, Current perspectives on tree nut allergy: a review, *J. Asthma Allergy* 11 (2018) 41–51.
- [16] V.L. McWilliam, K.P. Perrett, T. Dang, R.L. Peters, Prevalence and natural history of tree nut allergy, *Ann. Allergy Asthma Immunol.* 124 (2020) 466–472.
- [17] X. Weng, G. Gaur, S. Neethirajan, Rapid detection of food allergens by microfluidics ELISA-based optical sensor, *Biosensors* 6 (2016) 24.
- [18] S. Neethirajan, X. Weng, A. Tah, J. Cordero, K. Ragavan, Nano-biosensor platforms for detecting food allergens—New trends, Sensing and bio-sensing research 18 (2018) 13–30.
- [19] A.K. Pandey, R.K. Varshney, H.K. Sudini, M.K. Pandey, An improved enzyme-linked immunosorbent assay (ELISA) based protocol using seeds for detection of five major peanut allergens Ara h 1, Ara h 2, Ara h 3, Ara h 6, and Ara h 8, *Front. Nutr.* 6 (2019) 68.
- [20] R. Linacero, A. Sanchiz, I. Ballesteros, C. Cuadrado, Application of real-time PCR for tree nut allergen detection in processed foods, *Crit. Rev. Food Sci. Nutr.* 60 (2020) 1077–1093.
- [21] M. Prado, I. Ortea, S. Vial, J. Rivas, P. Calo-Mata, J. Barros-Velázquez, Advanced DNA- and protein-based methods for the detection and investigation of food allergens, *Crit. Rev. Food Sci. Nutr.* 56 (2016) 2511–2542.
- [22] L. Rotariu, F. Lagarde, N. Jaffrezic-Renault, C. Bala, Electrochemical biosensors for fast detection of food contaminants—trends and perspective, *TrAC, Trends Anal. Chem.* 79 (2016) 80–87.
- [23] W. Wang, J. Han, Y. Wu, F. Yuan, Y. Chen, Y. Ge, Simultaneous detection of eight food allergens using optical thin-film biosensor chips, *J. Agric. Food Chem.* 59 (2011) 6889–6894.
- [24] M. Peeters, B. van Grinsven, T.J. Cleij, K.L. Jiménez-Monroy, P. Cornelis, E. Pérez-Ruiz, G. Wackers, R. Thoelen, W. De Ceuninck, J. Lammertyn, P. Wagner, Label-free protein detection based on the heat-transfer method—A case study with the

- peanut allergen Ara h 1 and aptamer-based synthetic receptors, *ACS Appl. Mater. Interfaces* 7 (2015) 10316–10323.
- [25] R. Pilolli, L. Monaci, A. Visconti, Advances in biosensor development based on integrating nanotechnology and applied to food-allergen management, *TrAC, Trends Anal. Chem.* 47 (2013) 12–26.
- [26] D. Xu, X. Huang, J. Guo, X. Ma, Automatic smartphone-based microfluidic biosensor system at the point of care, *Biosens. Bioelectron.* 110 (2018) 78–88.
- [27] K. Bremer, B. Roth, Fibre optic surface plasmon resonance sensor system designed for smartphones, *Opt Express* 23 (2015) 17179–17184.
- [28] Y. Liu, Q. Liu, S. Chen, F. Cheng, H. Wang, W. Peng, Surface plasmon resonance biosensor based on smart phone platforms, *Sci. Rep.* 5 (2015), 12864.
- [29] C. Lertvachirapaiboon, A. Baba, K. Shinbo, K. Kato, A smartphone-based surface plasmon resonance platform, *Anal. Methods* 10 (2018) 4732–4740.
- [30] H. Guner, E. Ozgur, G. Kokturk, M. Celik, E. Esen, A.E. Topal, S. Ayas, Y. Uludag, C. Elbuken, A. Dana, A smartphone based surface plasmon resonance imaging (SPRI) platform for on-site biodection, *Sensor. Actuator. B Chem.* 239 (2017) 571–577.
- [31] M.Y. Pan, K.L. Lee, S.C. Lo, P.K. Wei, Resonant position tracking method for smartphone-based surface plasmon sensor, *Anal. Chim. Acta* 1032 (2018) 99–106.
- [32] Z. Fan, Z. Geng, W. Fang, X. Lv, Y. Su, S. Wang, H. Chen, Smartphone biosensor system with multi-testing unit based on localized surface plasmon resonance integrated with microfluidics chip, *Sensors* (2020) 20.
- [33] J. Zhou, Q. Qi, C. Wang, Y. Qian, G. Liu, Y. Wang, L. Fu, Surface plasmon resonance (SPR) biosensors for food allergen detection in food matrices, *Biosens. Bioelectron.* 142 (2019), 111449.
- [34] J. Ashley, M. Piekarska, C. Segers, L. Trinh, T. Rodgers, R. Willey, I.E. Tothill, An SPR based sensor for allergens detection, *Biosens. Bioelectron.* 88 (2017) 109–113.
- [35] M.G. Bremer, N.G. Smits, W. Haasnoot, Biosensor immunoassay for traces of hazelnut protein in olive oil, *Anal. Bioanal. Chem.* 395 (2009) 119–126.
- [36] A.S. Tsagkaris, J.L. Nelis, G. Ross, S. Jafari, J. Guercetti, K. Kopper, Y. Zhao, K. Rafferty, J.P. Salvador, D. Migliorelli, Critical assessment of recent trends related to screening and confirmatory analytical methods for selected food contaminants and allergens, *TrAC, Trends Anal. Chem.* 121 (2019), 115688.
- [37] Y. Liu, S. Chen, Q. Liu, J.F. Masson, W. Peng, Compact multi-channel surface plasmon resonance sensor for real-time multi-analyte biosensing, *Opt Express* 23 (2015) 20540–20548.
- [38] Q. Liu, Y. Liu, S. Chen, F. Wang, W. Peng, A low-cost and portable dual-channel fiber optic surface plasmon resonance system, *Sensors* 17 (2017).
- [39] S.D. Soelberg, T. Chinowsky, G. Geiss, C.B. Spinelli, R. Stevens, S. Near, P. Kauffman, S. Yee, C.E. Furlong, A portable surface plasmon resonance sensor system for real-time monitoring of small to large analytes, *J. Ind. Microbiol. Biotechnol.* 32 (2005) 669–674.
- [40] A. Sonato, M. Agostini, G. Ruffato, E. Gazzola, D. Liuni, G. Greco, M. Travaglati, M. Cecchini, F. Romanato, A surface acoustic wave (SAW)-enhanced grating-coupling phase-interrogation surface plasmon resonance (SPR) microfluidic biosensor, *Lab Chip* 16 (2016) 1224–1233.
- [41] E. Ouellet, C. Lausted, T. Lin, C.W. Yang, L. Hood, E.T. Lagally, Parallel microfluidic surface plasmon resonance imaging arrays, *Lab Chip* 10 (2010) 581–588.
- [42] C.-S. Chuang, C.-Y. Wu, P.-H. Juan, N.-C. Hou, Y.-J. Fan, P.-K. Wei, H.-J. Sheen, LMP1 gene detection using a capped gold nanowire array surface plasmon resonance sensor in a microfluidic chip, *Analyst* 145 (2020) 52–60.
- [43] C. Xiao, J. Eriksson, A. Suska, D. Filippini, W.C. Mak, Print-and-stick unibody microfluidics coupled surface plasmon resonance (SPR) chip for smartphone imaging SPR (Smart-ISRP), *Anal. Chim. Acta* 1201 (2022), 339606.
- [44] G.M.S. Ross, G.I. Salentijn, M.W.F. Nielen, A critical comparison between flow-through and lateral flow immunoassay formats for visual and smartphone-based multiplex allergen detection, *Biosensors* 9 (2019).
- [45] G.M.S. Ross, D. Filippini, M.W.F. Nielen, G.I. Salentijn, Interconnectable solid-liquid protein extraction unit and chip-based dilution for multiplexed consumer immunodiagnosics, *Anal. Chim. Acta* 1140 (2020) 190–198.
- [46] J. Mocak, A.M. Bond, S. Mitchell, G. Scollary, A statistical overview of standard (IUPAC and ACS) and new procedures for determining the limits of detection and quantification: application to voltammetric and stripping techniques (technical report), *Pure Appl. Chem.* 69 (1997) 297–328.
- [47] S. Rebe Raz, H. Liu, W. Norde, M.G. Bremer, Food allergens profiling with an imaging surface plasmon resonance-based biosensor, *Anal. Chem.* 82 (2010) 8485–8491.